

General nonlinear Hall current in magnetic insulators beyond the quantum anomalous Hall effect

Daniel Kaplan, Tobias Holder, and Binghai Yan*

Department of Condensed Matter Physics, Weizmann Institute of Science, Rehovot 7610001, Israel
(Dated: September 21, 2022)

Can a generic magnetic insulator exhibit a Hall current? The quantum anomalous Hall effect (QAHE) is one example of an insulating bulk carrying a quantized Hall conductivity and other insulators (with zero Chern number) present zero Hall conductance in the linear response regime. Here, we find that a general magnetic insulator possesses a nonlinear Hall conductivity quadratic to the electric field if the system breaks inversion symmetry. This conductivity originates from an induced orbital magnetization due to virtual interband transitions. We identify three contributions to the wavepacket motion, a velocity shift, a positional shift, and a Berry curvature renormalization. In contrast to the crystalline solid, we find that this nonlinear Hall conductivity vanishes for Landau levels of a 2D electron gas, indicating a fundamental difference between the QAHE and the Integer quantum Hall effect.

Introduction.— Understanding electric conduction of insulators is fundamental to condensed matter physics. For example, the quantum Hall effect is a unique realization of a 2D topological insulating phase of matter, with distinct experimental signatures [1–4], notably a quantized Hall conductance σ^{xy} which adheres to the quantized value $\frac{e^2}{h}$ with astonishing precision, up to at least 10^{-10} [5, 6]. It has been known since the early days of the quantum Hall effect [7] that the quantization of σ_{xy} is related to the Berry curvature in a periodic system, with the robustness of the quantization discussed in several works [8–10]. As a close cousin, the quantum anomalous Hall effect (QAHE) refers to the appearance of a quantized Hall conductivity in 2D systems even in the absence of a magnetic field [11–13]. First proposed by Haldane [14], the QAHE requires the breaking of time-reversal symmetry (TRS) in the crystal system characterized by a Chern number C_N for the occupied bands. Consequently, a calculation at linear order yields for the Hall conductivity $\sigma^{xy} = C_N \frac{e^2}{h}$ [15, 16]. The QAHE has been experimentally realized in several systems, notably magnetically doped thin-films of topological insulators [17, 18], stoichiometric magnetic topological insulators [19], and recently in Moiré superlattices [20, 21]. However, in contrast to the quantum Hall effect, careful experiments on the QAHE find a less precisely quantized Hall conductivity, with precision of 0.01% [18] and 0.1% [20] respectively.

While it is well established that the Hall conductivity is exactly quantized at linear order [7], in this letter we find that an intrinsic nonlinear conductivity can appear at finite bias for generic magnetic insulators. These nonlinear effects are due to virtual interband transitions, which have been shown to appear beyond linear response even in insulators [22, 23]. This is a testament to the fact that the Hall conductivity is a response function which can depend on the applied bias and which is not identical in physical content to the Chern number of the ground state [24]. An intuitive picture of these interband transitions is shown in Fig. 1: The quasiparticle response can

be modified by shifts in velocity, shifts in position, and by a renormalization of the Berry curvature. In the following, we derive the nonlinear conductivity in quantum perturbation theory, and formulate our main result as a correction to the semiclassical equations of motion. An immediate question is why such effects are absent in the integer quantum Hall effect. The reason is that the Berry phase is entirely created by the applied magnetic field and thus extrinsic and independent of the underlying band structure, which is fully renormalized and transformed into Landau levels. Thus, no correction to the Berry phase is expected from band structure terms, and indeed as we will show, the higher-order terms considered here are rendered zero for a Landau level dispersion.

Theory.— As is well known, an applied perturbation does not usually commute with the band Hamiltonian H_0 and will induce interband transitions in terms of the unperturbed eigenvalues of H_0 . Thus, a wavepacket initially centered on a single Bloch periodic state $|W\rangle = \int d\mathbf{k} a_n(\mathbf{k}) |n\mathbf{k}\rangle$ at $t = 0$, will evolve to be a linear combination containing contributions of many bands [25, 26]. In the Kubo formalism this is reflected in the appearance of resonant contributions which are broadened by the finite quasiparticle lifetime τ . We consider an insulator with broken inversion and time-reversal symmetries, i. e. it holds for the dispersion $\varepsilon_n(\mathbf{k}) \neq \varepsilon_n(-\mathbf{k})$. The uniform ($\mathbf{q} \rightarrow 0$) electric field $\mathbf{E} = \mathbf{E}_0 e^{i\omega t}$ is introduced via its vector potential $\mathbf{A}(t) = \frac{\mathbf{E}_0 e^{i\omega t}}{i\omega}$. By minimal coupling the Bloch-periodic Hamiltonian transforms as $H_0(\mathbf{k}) \rightarrow H_0(\mathbf{k} - e\mathbf{A})$. The current operator is given by $J^c = \frac{\delta H}{\delta A^c}$. Up to \mathbf{A}^2 this yields

$$J^c = -ev^c + e^2 \sum_a \mathbf{A}^a w^{ac} - \frac{e^3}{2} \sum_{a,b} \mathbf{A}^a \mathbf{A}^b u^{abc}, \quad (1)$$

where $v^a = \partial_a H_0$, $w^{ab} = \partial_a \partial_b H_0$, $u^{abc} = \partial_a \partial_b \partial_c H_0$ and $\partial_a = \frac{\partial}{\partial k_a}$. The evaluation of the total current is then

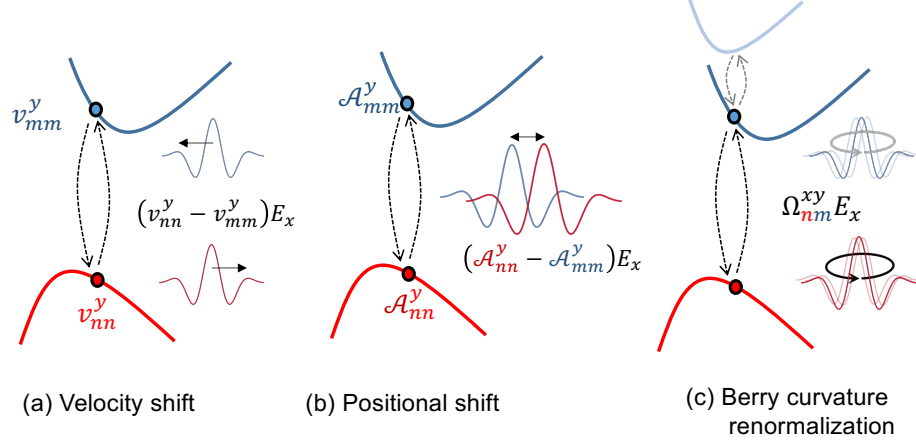


Figure 1. **Illustration of corrections to the AHE conductivity in the presence of an electric field (E_x).** (a) Velocity shift of the wave packet due to transition between the occupied (n) and unoccupied (m) bands. (b) Positional shift of a wavepacket due to interband transitions. (c) Berry curvature renormalization by the third bands. All three contributions (see Eqs. 4, 5 and 6), which are linear in E_x , are non-zero for a generic multiband dispersion which breaks both inversion and time-reversal symmetries.

carried out using a Green's function approach [27, 28],

$$\langle j^c \rangle = -i \int \frac{d^d k}{(2\pi)^d} \int \frac{d\Omega}{2\pi} \text{Tr} (J^c G^<(k, \Omega)). \quad (2)$$

Here $G^<$ is the lesser Green's function [28]. The lesser Green's function is found through a solution to the Dyson equation, giving $G^< = (1 + G^r \Sigma^r) G_0^< (1 + G^a \Sigma^a)$, and $G^r = G_0^r (1 + \Sigma^r G^r)$, $G^a = G_0^a (1 + \Sigma^a G^a)$. In the usual manner [27], Dyson's equations are solved perturbatively. Since the electromagnetic coupling is Hermitian, $\Sigma^r = \Sigma^a = -\sum J^c \mathbf{A}^c(\omega)$, and $G^{r/a} = G_0^{r/a} \sum_{n=0}^{\infty} (\Sigma^{r/a} G_0^{r/a})^n$, and correspondingly $G^< = \sum_{n=0}^{\infty} (\Sigma^r G_0^r)^n G_0^< \sum_{m=0}^{\infty} (\Sigma^a G_0^a)^m$. The diagrammatic expansion of $G^<$ has recently been developed yielding the complete response at 2^{nd} order in \mathbf{A} [29, 30]. In the Bloch basis $|n\mathbf{k}\rangle$ the unperturbed Green's functions are $G_{0,nm}^r(\Omega) = \frac{\delta_{nm}}{\Omega - \varepsilon_n + i\tau^{-1}}$, $G_{0,nm}^a(\Omega) = \frac{\delta_{nm}}{\Omega - \varepsilon_n - i\tau^{-1}}$, $G_{0,nm}^<(\Omega) = 2\pi i \delta_{nm} f_n \delta(\Omega - \varepsilon_n)$. Here f_n is the Fermi occupation factor. We begin by considering $\mathbf{A}(\omega)$ at finite frequency, and then taking the limit $\omega \rightarrow 0$. Crucially, the $\omega \rightarrow 0$ pole is avoided by retardation in the form of $\omega \rightarrow \omega + \frac{i}{\tau}$. The expansion of $G^<$ will contain a pole in the sum of frequencies, which is shifted by $\omega + (-\omega) \rightarrow \omega + (-\omega) + \frac{2i}{\tau}$. The result is then evaluated in the $\tau \rightarrow \infty$ limit. The expansion for the lifetime-free (τ^0) contribution is detailed in the Supplementary Information [31]. The full expansion for all orders of τ and the general expressions are presented in Ref. [32]. For concreteness, we present the case $\mathbf{E}_0 = (E_x, 0, 0)$ and focus on two-dimensional systems. At order τ^0 , and up to order $\mathcal{O}(\mathbf{A}^2)$ the transverse conductivity σ^{xy} reads,

$$\sigma^{xy} = \frac{e^2}{\hbar} \sum_{n \in \text{occ.}} \int \frac{d^2 k}{(2\pi)^2} \left[\Omega_{nn}^{xy} + eE_x (I_1 + I_2 + I_3)_{nn}^{xy} \right] \quad (3)$$

$$(I_1)_{nn}^{xy} = [\varepsilon^{-2} \mathcal{A}^x, \Delta^y \mathcal{A}^x]_{nn} - [\varepsilon^{-2} \mathcal{A}^y, \Delta^x \mathcal{A}^x]_{nn} \quad (4)$$

$$(I_2)_{nn}^{xy} = 2 [\varepsilon^{-1} \mathcal{A}^x, S^{xy}] - 2 [\varepsilon^{-1} \mathcal{A}^y, S^{xx}] \quad (5)$$

$$(I_3)_{nn}^{xy} = i [\varepsilon^{-1} \mathcal{A}^x, [\mathcal{A}^x, \mathcal{A}^y]]_{nn}. \quad (6)$$

Here, we introduced compact notation: $[A, B]_{nm} = \sum_{l \neq n, m} A_{nl} B_{lm} - (B \leftrightarrow A)$, and $\Delta_{nm}^{x,y} = v_{nn}^{x,y} - v_{mm}^{x,y}$, which is resolved using the Hadamard product, i.e., $(A \Delta^{x,y})_{nm} = A_{nm} \Delta_{nm}^{x,y}$. $\varepsilon_n(\mathbf{k})$ is the energy of the n -th Bloch band, at momentum \mathbf{k} , and is also inserted in the expression in the Hadamard form. $\mathcal{A}^{x,y}$ is the non-Abelian Berry connection, defined as usual $\langle n | \hat{\mathbf{r}} | m \rangle = \mathcal{A}_{nm}$, where \mathbf{r}_{nm} is the position operator.

In writing Eq. (3), we split the nonlinear conductivity into three physically distinguishable response types. Namely, I_1 is associated with a velocity shift, Δ_{nm}^{α} , while I_3 describes a renormalization of the Berry curvature. Each of these is individually gauge invariant (see SI), and is the result of residual processes from the optical, high-frequency limit. The velocity shift I_1 has a form similar to the injection current seen in TRS-broken systems at high frequencies [30, 33]. I_3 is a purely multi-band object seen at higher-order response. In the case of a coupling between magnetic and electric fields, it is related to the non-topological part of the magneto-electric polarizability [34]. Finally, I_2 involves a tensor S^{xy} which is related to the shift-vector found in optical response [35]. This quantity is defined as,

$$S_{nm}^{\alpha\beta} = (1 - \delta_{nm}) \left(\lambda_{nm}^{\alpha\beta} - \frac{i}{2} (\mathcal{A}_{nm}^{\alpha} \delta_{nm}^{\beta} + \mathcal{A}_{nm}^{\beta} \delta_{nm}^{\alpha}) \right), \quad (7)$$

$$\lambda_{nm}^{\alpha\beta} = \frac{i}{2} (\langle n | \partial_{\alpha} \partial_{\beta} m \rangle - \langle \partial_{\alpha} \partial_{\beta} n | m \rangle). \quad (8)$$

$\lambda_{nm}^{\alpha\beta}$ presents a higher derivative on the wavefunction, which results from the resolution of $\partial_{\alpha} \mathcal{A}_{nm}^{\beta}$. $\delta_{nm}^{\alpha} =$

$\mathcal{A}_{nn}^\alpha - \mathcal{A}_{mm}^\alpha$ which encodes a real-space shift of the wavefunction center [36] also appears, with the latter entering via a Hadamard product, thus rendering $S^{\alpha\beta}$ manifestly gauge covariant: $S_{nm}^{\alpha\beta} \rightarrow e^{i\theta_{nm}(\mathbf{k})} S_{nm}^{\alpha\beta}$, under the $U(1)^N$ gauge transformation, with the Bloch wavefunctions transforming as $|\psi_{n\mathbf{k}}\rangle \rightarrow e^{i\theta_n(\mathbf{k})} |\psi_{n\mathbf{k}}\rangle$. The commutator structure ensures the gauge invariance of the entire expression for σ^{xy} . A detailed proof of the gauge invariance under a $U(1)^N$ transformation for each of the terms is presented in the SI [31]. The appearance of $\Delta^{x,y}$ as well as $\delta^{x,y}$ in Eq. (6) shows the connection of these objects to expressions at finite frequency such as injection and shift currents [30, 37–39]. The second-order correction in Eq. (6) has several noteworthy properties:

Absence of longitudinal components.— The correction may be nonzero only in the direction perpendicular to the applied field, and only enters the transverse components of $\sigma^{\alpha\beta}$ (in any dimension). This is of course due to the fact that the correction is related to the Berry curvature, which ensures that the resultant current is always perpendicular to the perturbation. Consequently, the correction does not violate charge conservation nor does it produce a longitudinal response which would require a finite Fermi surface [40].

Multiband nature – Inspection of Eqs. (4)–(6) reveals that the in-gap conductivity is generated by interband processes, which are due to virtual transitions between occupied and unoccupied bands. This is a direct result of the commutator structure because $f_n[A, B]_{nn} = f_{nm}A_{nm}B_{mn}$ where $f_{nm} = f_n - f_m$. The latter vanishes if both states are occupied or empty. Since Ω_{nn}^z can be projected into a single-band, it appears at linear order. But corrections to this are manifestly multi-band objects, involving direct probes of the states through $\Delta_{nm}^\alpha, \varepsilon_{nm}, S_{nm}^{\alpha\beta}$. The presence of the shift tensor $S_{nm}^{\alpha\beta}$ suggests a property which is encoded in at least two bands, as the commutator in which it appears restricts $n \neq m$. Furthermore, we note the presence of a higher-order multi-band term, $[A^x \varepsilon^{-1}, \Omega^z]_{nn}$, which is $(I_3)_{nn}$ in Eq. (6). To parse this object, one evaluates Ω_{nm}^z , where $n \neq m$. Using the definition of the commutator, however, $[A, B]_{nm} = \sum_{l \neq n, m} A_{nl}B_{lm} - (a \leftrightarrow B)$. From this, it follows that this term only exists for three bands or more. In the two band limit, the commutator can be directly evaluated to be $[A, B]_{12} = \sum_{l \neq 1, 2} A_{1l}B_{l2} - (A \leftrightarrow B) = 0$, as the sum cannot extend over *any* intermediate state. This term represents, therefore, a unique signature of a quantum process which involves interband transitions between two principle bands – occupied and empty – with an assisting interim third band.

Symmetries.— The correction to the anomalous Hall conductivity strongly depends on the underlying symmetry of the crystal lattice. Firstly, a general requirement for the appearance of intrinsic in-gap responses is the breaking of time-reversal symmetry (TRS). Since this effect is quadratic in the electric field, inversion symmetry

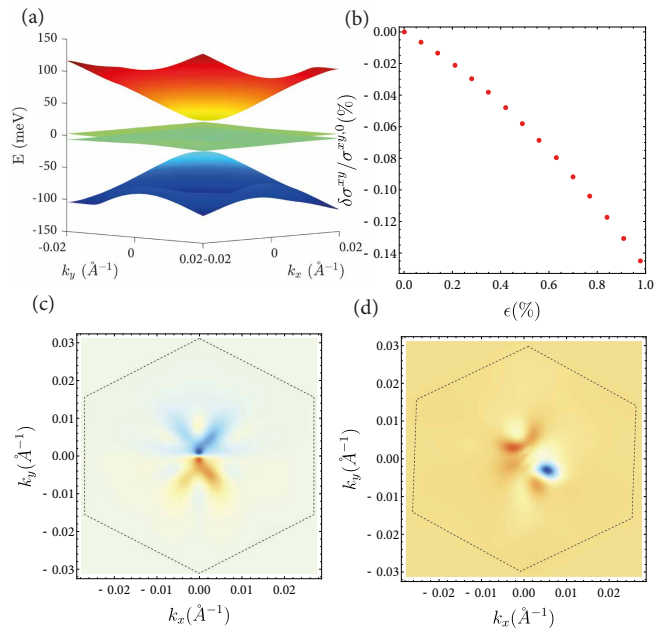


Figure 2. **Nonlinear correction to the anomalous Hall in TBG.** (a) Band structure of twisted bilayer graphene for $\theta \sim 1.05^\circ$. Remote dispersive bands contribute to the interband correction, which vanishes in the single-band limit. (b) Magnitude of the correction to the AHC $\sigma^{xy,0} = \frac{e^2}{h}$ as a function of applied uniaxial strain ϵ in TBG. (c-d) Momentum space distribution of $\delta\sigma^{xy}$ for $\epsilon = 0$ (c) and $\epsilon = 0.8\%$ in (d).

(P) must be broken as well. The symmetry discussion is simplified by considering the correction as a *second-order* Hall conductivity. We define $\sigma^{xx;y} = \frac{\delta^2 j_y}{\delta E_x \delta E_x}$. Eqs. (4)–(6) show that the Hall part of the tensor $\sigma^{ab;c}$ takes the form $\sigma^{aa;c}$. Applying the von Neumann principle [41], we find that for all rotational symmetries $C_{n,z}$, $n \geq 2$, $\sigma^{aa;c}$ vanishes identically. In 3D (or higher), other components of the response tensor are permitted, e.g. of the form $\sigma^{xx;z}$. The emergence of a longitudinal in-gap current is restricted by the presence of point-group symmetries. In the case of C_{3z} , for example, $\sigma^{xx;y} = -\sigma^{yy;y}$, but since the correction vanishes for $\sigma^{yy;y}$, the Hall response is null as well.

Twisted bilayer graphene.— As a candidate system to test our results, we suggest to use strained twisted bilayer graphene (TBG) [42–45]. As previously seen in the case of resonant optical conductivity [35], in TBG second-order electrical responses can become exceptionally large due to the large phase space for transitions between flat bands. We model a time-reversal breaking state of TBG by considering the Bistritzer-MacDonald [42] continuum model for a single valley and spin of TBG at a twist angle of $\theta = 1.05^\circ$. This corresponds to experimental measurements of TBG in the ferromagnetic, 3/4 filled state [20, 46], in a series of cascading symmetry-broken states in this system [47, 48]. This phase is topological

with a Chern number $C_N = 1$. In a sample, the TBG is usually placed on top of a layer of hBN [49, 50], which breaks inversion symmetry. This can be modelled by introducing a staggered potential $\Delta = 17\text{meV}$ [45]. Since TBG on top of hBN still retains a C_{3z} -symmetry, the correction considered here remains zero. This is shown in Fig. 2(b). Fig. 2(c) also reveals that the momentum distribution of the correction is anti-symmetric within the mini Brillouin zone (mBZ) and thus vanishes after integration. However, introducing strain breaks C_{3z} , rendering the correction in Eq. (3) nonzero, as seen in Fig. 2(d), with the mBZ modified as well. The deviation from $\sigma_0^{xy} = \frac{e^2}{h}$ increases with increasing strain. Using a typical strain amplitude of $\epsilon \sim 0.65\%$ [51], and electric field strengths of $E = 300\text{Vm}^{-1}$, it reaches a value of 0.1%, which is comparable to the deviation from perfect quantization in recent experiments [20].

Semiclassical interpretation.— The structure of the correction permits the following semiclassical form. We define the electric field-induced shift tensors,

$$\mathbf{v}_E^a = e \frac{\mathcal{A}^a \Delta^b}{\epsilon} E_b, \quad \mathbf{S}_E^a = e \mathbf{S}^{ab} E_b, \quad \Omega_E = e \Omega^{ab} E_b, \quad (9)$$

Where all terms enter as Hadamard products. In band basis, these objects are translated as $\mathbf{v}_E^a = \sum_b \frac{e}{\epsilon_{nm}} \mathcal{A}_{nm}^a \Delta_{nm}^b E_b$. This can be carried out analogously for all terms. The semi-classical anomalous current at second order can then be written as

$$\mathbf{j} = \frac{e^2}{\hbar} \sum_{n \in \text{occ.}} \mathbf{E} \times \int \frac{d^2k}{(2\pi)^2} \left(\Omega_{nn} + \left[\frac{\mathcal{A}}{\epsilon} \times \mathbf{V} \right]_{nn} \right). \quad (10)$$

Here, $\mathbf{V}_E^a = \mathbf{v}_E^a + \mathbf{S}_E^a + \Omega_E^a$. The cross product is to be interpreted as usual [15, 52], such that $\left[\frac{\mathcal{A}}{\epsilon} \times \mathbf{V} \right]_{nn} = \sum_{m \in \text{unocc.}} \epsilon^{abc} \frac{\mathcal{A}_{nm}^b}{\epsilon_{nm}} \mathbf{V}_{mn,E}^c - (n \leftrightarrow m)$. Here ϵ^{abc} is the Levi-Civita symbol. This partition into three pieces is identical in content to the previous decomposition into I_1, I_2, I_3 in Eq. (3). $\frac{\mathbf{V}_E^a}{\hbar}$ carries units of velocity, meaning that it is the velocity of the (instantaneous) charge displacement upon application of the external electric field \mathbf{E} . At first order, this displacement modifies the position operator through a change in the charge dipole. At second order in the applied field, this deformation couples back to the position operator, resulting in a correction to the anomalous velocity, now effectively quadratic in the applied field. The weight ϵ_{nm}^{-1} attached to the position operator reflects the quantum-perturbative expansion, since the \mathbf{V}^a is now explicitly *inter-band*, and the transitions to the neighboring bands are suppressed by the energy gap. The single band limit can be recovered in the limit where all unoccupied bands are infinitely separated from the top of the valence band such that $\epsilon_{nm} \rightarrow \infty$. In this limit $\frac{\mathcal{A}}{\epsilon}$ vanishes, and the usual anomalous velocity is recovered. A visualization of the momentum-space structure of $\text{Re}(\mathbf{V})$ using a simplified two band model can be found in the SI [31].

Robustness of the integer quantum Hall effect.— The precise quantization of the conductivity σ^{xy} of the integer quantum hall effect for a 2D electron gas can be understood in the absence of any higher-order corrections at finite bias. To show that our correction vanishes identically for Landau levels, consider the Hamiltonian of an electron gas in the Landau gauge, $\mathbf{A} = (0, -Bx, 0)$,

$$H = \frac{p_{x'}^2}{2M} + \frac{M\omega_c^2 x'^2}{2}. \quad (11)$$

Here as usual $\omega_c = \frac{eB}{M}$, and $x' = x + \frac{\hbar k_y}{eB}$. We shall show that the quantization of the Hall conductivity is guaranteed by the ladder operator structure. The velocity matrix elements in the Landau level basis are,

$$v_x = \frac{\partial H}{\partial \pi_{x'}} = \frac{p_{x'}}{M} = i\sqrt{\frac{\hbar\omega_c}{2M}}(a^\dagger - a), \quad (12)$$

$$v_y = \frac{\partial H}{\partial \pi_y} = \omega_c x' = \frac{\omega_c l_B}{\sqrt{2}}(a + a^\dagger). \quad (13)$$

We define the latter operators $a = \frac{1}{\sqrt{2m\hbar\omega_c}}(ip_{x'} + M\omega_c x')$ and $l_B = \sqrt{\frac{\hbar}{eB}}$. For Landau levels, $\epsilon_n = \hbar\omega_c(n + 1/2)$, $a^\dagger |n\rangle = \sqrt{n+1} |n+1\rangle$, and $a |n\rangle = \sqrt{n} |n-1\rangle$. The expectation values become $\langle n | v_x | m \rangle = i \frac{\hbar}{\sqrt{2M}l_B} (\sqrt{m+1}\delta_{n,m+1} - \sqrt{m}\delta_{n,m-1})$, $\langle n | v_y | m \rangle = \frac{\omega_c l_B}{\sqrt{2}} (\sqrt{m+1}\delta_{n,m+1} + \sqrt{m}\delta_{n,m-1})$. The quantization of the linear conductivity is directly related to the ladder structure of operator algebra in the integer quantum Hall fluid. A demonstration of this property is relegated to the SM. However, the fact that the ladder operators only connect Landau levels with energy differences $\Delta\epsilon = \pm\hbar\omega_c$ can be used to show that *all* higher-order corrections vanish for the 2D electron gas at high magnetic field. At 2nd order, the relevant diagrams of the quantum perturbative calculation give two contributions at order τ^0 (all other terms vanish in the gapped phase identically) [32]. For the Hall response tensor $\sigma^{xx;y}$,

$$\begin{aligned} \sigma^{xx;y} &= \frac{e^3}{\hbar^2} \sum_n f_n [-2 [\epsilon^{-3} w^{xx}, v_y]_{nn} - [\epsilon^{-3} v^x, w^{xy}]_{nn}] \\ &+ \frac{e^3}{\hbar^2} \sum_{n,m} \left[-4 \frac{f_{nm}}{\epsilon_{nm}\epsilon_{nl}^3} v_{nm}^x v_{ml}^x v_{ln}^y \right. \\ &\left. - 2 \frac{f_{nm}}{\epsilon_{nm}^2 \epsilon_{nl}^2} v_{nm}^x v_{ml}^x v_{ln}^y - \frac{f_{nm}}{\epsilon_{nm}^3 \epsilon_{nl}} v_{nm}^x v_{ml}^x v_{ln}^y \right]. \quad (14) \end{aligned}$$

The elimination of the first two commutators in Eq. (14) is due to the free fermion dispersion of the Landau levels giving $w_{nm}^{ab} = \langle n | \left[\frac{\partial^2 H}{\partial \pi_a \partial \pi_b} \right] | m \rangle \propto \delta_{nm}$ since the underlying dispersion is quadratic in Eq. (11). The commutator $[A, B]_{nn}$ contains only off-diagonal components of A_{nm}, B_{nm} . Consequently, since $w_{nm}^{ab} = 0$ for any $a, b, n \neq m$ this contribution vanishes. We are left with

the triple product $v_{nm}^x v_{ml}^x v_{ln}^y$. By applying the ladder structure for $v_{nm}^{x,y}$ the following combinations appears: $\delta_{n,m\pm 1} \delta_{m,l\pm 1} \delta_{l,n\pm 1}$ [53]. By applying, e.g., the middle Kronecker delta, we have the condition that $n = l \pm 1 \pm 1$, and $n = l \mp 1$. Clearly, there exists no l, n that satisfies this constraint. This results in $\sigma^{x,x;y} = 0$ regardless of the exact structure of the Hamiltonian, provided the algebra of the ladder operators is preserved. The generalization of the above can be made by considering that n -th order response will contain an $n+1$ product of velocity operators $v_{m_1 m_2}^x v_{m_2 m_3}^x v_{m_3 m_4}^x \dots v_{m_n m_1}^y$, which produces the condition that $\delta_{n_1 n_2 \pm 1} \delta_{n_2 n_3 \pm 1} \delta_{n_3 n_4 \pm 1} \dots$ which yields zero for the real part of the current at any order. The only nonzero combination for which band indices can be selected appears at order $n = 1$ corresponding to linear response, which gives the quantized integer Hall conductivity.

Conclusions.— We have shown that in general magnetic insulators which break inversion, time reversal as well as rotational symmetries, a quadratic correction to the in-gap Hall conductivity appears. In a topological phase, this indicates that measurements at finite bias will deviate from the quantized value due to the presence of nonlinear corrections. As an example, we calculated the correction for strained twisted bilayer graphene, finding for the magnitude of the nonlinearity values which are comparable with the observed precision of the quantization in the recent experiment of Ref. [20]. Another experimental signature may appear in the non-reciprocal nature of the conductivity. Namely, in systems where the correction is observable we find that $\sigma^{xy} \neq -\sigma^{yx}$, and the sum $\sigma^{xy} + \sigma^{yx}$ can thus be treated as a proxy for the correction. Thirdly, the quantities derived here might be visible as non-linear powers in the $I - V$ curve.

Recent progress on nonlinearities in graphene superlattices [54] suggests that experiments at moderate finite bias on graphene-based systems are possible. By tuning the graphene superlattices to the QAH state and sweeping the bias, the nonlinear corrections, as well as the non-reciprocity they produce might be accessible. In addition, the sensitivity of the effect to strain suggests an electro-mechanical setup in which a controlled application of tensile stress is employed in order to modify the Hall conductivity (at finite bias). We note that systems with C_{3z} symmetry, such as doped Bi_2Se_3 [17] do not exhibit this correction due to the symmetry restriction. Our results might be relevant in understanding why experiments on systems with rotational symmetries observe a much more precisely quantized QAHE [18, 55]. Related to that, the reasoning presented here raises the question whether third or even higher order corrections are non-vanishing even if a QAH system has inversion and C_3 symmetry. Our result establishes a concrete difference in the quantization of the QAHE compared to the IQHE, which suggests that using QAHE systems for metrology depends on subtleties related to the crystal systems, symmetries and the magnitude of the applied bias. Our results predict a

striking phenomenon that a generic insulator can present a nonlinear current response in the dc limit.

We thank Ady Stern and Xi Dai for useful discussions. B.Y. acknowledges the financial support by the European Research Council (ERC Consolidator Grant No. 815869, “NonlinearTopo”) and Israel Science Foundation (ISF No. 2932/21). D. Kaplan appreciates support from the Weizmann Institute Sustainability and Energy Research Initiative.

* binghai.yan@weizmann.ac.il

- [1] K. v. Klitzing, G. Dorda, and M. Pepper, New method for high-accuracy determination of the fine-structure constant based on quantized hall resistance, *Phys. Rev. Lett.* **45**, 494 (1980).
- [2] K. von Klitzing, The quantized hall effect, *Rev. Mod. Phys.* **58**, 519 (1986).
- [3] T. Senthil, Symmetry-Protected Topological Phases of Quantum Matter, *Annu. Rev. Condens. Matter Phys.* **6**, 299 (2015), arXiv:1405.4015 [cond-mat.str-el].
- [4] T. H. Hansson, M. Hermanns, S. H. Simon, and S. F. Viefers, Quantum Hall physics: Hierarchies and conformal field theory techniques, *Reviews of Modern Physics* **89**, 025005 (2017), arXiv:1601.01697 [cond-mat.str-el].
- [5] F. Schopfer and W. Poirier, Testing universality of the quantum hall effect by means of the wheatstone bridge, *Journal of Applied Physics* **102**, 054903 (2007), <https://doi.org/10.1063/1.2776371>.
- [6] W. Poirier and F. Schopfer, Resistance metrology based on the quantum Hall effect, *European Physical Journal Special Topics* **172**, 207 (2009).
- [7] D. J. Thouless, M. Kohmoto, M. P. Nightingale, and M. den Nijs, Quantized Hall Conductance in a Two-Dimensional Periodic Potential, *Phys. Rev. Lett.* **49**, 405 (1982).
- [8] B. L. Altshuler, D. Khmel'nitzkii, A. I. Larkin, and P. A. Lee, Magnetoresistance and hall effect in a disordered two-dimensional electron gas, *Phys. Rev. B* **22**, 5142 (1980).
- [9] J. E. Avron, R. Seiler, and B. Simon, Homotopy and quantization in condensed matter physics, *Phys. Rev. Lett.* **51**, 51 (1983).
- [10] G. Zala, B. Narozhny, and I. Aleiner, Interaction corrections to the hall coefficient at intermediate temperatures, *Phys. Rev. B* **64**, 201201 (2001).
- [11] C.-X. Liu, S.-C. Zhang, and X.-L. Qi, The quantum anomalous hall effect: Theory and experiment, *Annual Review of Condensed Matter Physics* **7**, 301 (2016), <https://doi.org/10.1146/annurev-conmatphys-031115-011417>.
- [12] K. He, Y. Wang, and Q.-K. Xue, Topological materials: Quantum anomalous hall system, *Annual Review of Condensed Matter Physics* **9**, 329 (2018), <https://doi.org/10.1146/annurev-conmatphys-033117-054144>.
- [13] C.-Z. Chang, C.-X. Liu, and A. H. MacDonald, Quantum anomalous Hall effect, arXiv e-prints, arXiv:2202.13902 (2022), arXiv:2202.13902 [cond-mat.mes-hall].
- [14] F. D. M. Haldane, Model for a quantum hall effect without

- landau levels: Condensed-matter realization of the "parity anomaly", *Phys. Rev. Lett.* **61**, 2015 (1988).
- [15] D. Xiao, M.-C. Chang, and Q. Niu, Berry phase effects on electronic properties, *Rev. Mod. Phys.* **82**, 1959 (2010), arXiv:0907.2021 [cond-mat.mes-hall].
- [16] N. Nagaosa, J. Sinova, S. Onoda, A. H. MacDonald, and N. P. Ong, Anomalous Hall effect, *Rev. Mod. Phys.* **82**, 1539 (2010), arXiv:0904.4154 [cond-mat.mes-hall].
- [17] C.-Z. Chang, J. Zhang, X. Feng, J. Shen, Z. Zhang, M. Guo, K. Li, Y. Ou, P. Wei, L.-L. Wang, Z.-Q. Ji, Y. Feng, S. Ji, X. Chen, J. Jia, X. Dai, Z. Fang, S.-C. Zhang, K. He, Y. Wang, L. Lu, X.-C. Ma, and Q.-K. Xue, Experimental Observation of the Quantum Anomalous Hall Effect in a Magnetic Topological Insulator, *Science* **340**, 167 (2013), arXiv:1605.08829 [cond-mat.mes-hall].
- [18] C.-Z. Chang, W. Zhao, D. Y. Kim, H. Zhang, B. A. Assaf, D. Heiman, S.-C. Zhang, C. Liu, M. H. Chan, and J. S. Moodera, High-precision realization of robust quantum anomalous hall state in a hard ferromagnetic topological insulator, *Nature materials* **14**, 473 (2015).
- [19] Y. Deng, Y. Yu, M. Z. Shi, Z. Guo, Z. Xu, J. Wang, X. H. Chen, and Y. Zhang, Quantum anomalous Hall effect in intrinsic magnetic topological insulator MnBi_2Te_4 , *Science* **367**, 895 (2020), arXiv:1904.11468 [cond-mat.mtrl-sci].
- [20] M. Serlin, C. L. Tschirhart, H. Polshyn, Y. Zhang, J. Zhu, K. Watanabe, T. Taniguchi, L. Balents, and A. F. Young, Intrinsic quantized anomalous Hall effect in a moiré heterostructure, *Science* **367**, 900 (2020), arXiv:1907.00261 [cond-mat.str-el].
- [21] T. Li, S. Jiang, B. Shen, Y. Zhang, L. Li, Z. Tao, T. Devakul, K. Watanabe, T. Taniguchi, L. Fu, J. Shan, and K. F. Mak, Quantum anomalous Hall effect from intertwined moiré bands, *Nature (London)* **600**, 641 (2021), arXiv:2107.01796 [cond-mat.mes-hall].
- [22] Y. Michishita and R. Peters, Effects of renormalization and non-Hermiticity on nonlinear responses in strongly correlated electron systems, *Phys. Rev. B* **103**, 195133 (2021), arXiv:2012.10603 [cond-mat.str-el].
- [23] D. Kaplan, T. Holder, and B. Yan, Nonvanishing Sub-gap Photocurrent as a Probe of Lifetime Effects, *Phys. Rev. Lett.* **125**, 227401 (2020), arXiv:2003.12582 [cond-mat.mes-hall].
- [24] T. Holder, Electrons flow like falling cats: Deformations and emergent gravity in quantum transport, arXiv, arXiv:2111.07782 (2021), arXiv:2111.07782 [cond-mat.mes-hall].
- [25] D. Culcer, Y. Yao, and Q. Niu, Coherent wave-packet evolution in coupled bands, *Phys. Rev. B* **72**, 085110 (2005), arXiv:cond-mat/0411285 [q-bio.OT].
- [26] M.-C. Chang and Q. Niu, TOPICAL REVIEW: Berry curvature, orbital moment, and effective quantum theory of electrons in electromagnetic fields, *Journal of Physics Condensed Matter* **20**, 193202 (2008).
- [27] G. Mahan, *Many-Particle Physics* (Springer, 1990).
- [28] R. A. Jishi, *Feynman diagram techniques in condensed matter physics* (Cambridge University Press, 2013).
- [29] D. E. Parker, T. Morimoto, J. Orenstein, and J. E. Moore, Diagrammatic approach to nonlinear optical response with application to Weyl semimetals, *Phys. Rev. B* **99**, 045121 (2019), arXiv:1807.09285 [cond-mat.str-el].
- [30] T. Holder, D. Kaplan, and B. Yan, Consequences of time-reversal-symmetry breaking in the light-matter interaction: Berry curvature, quantum metric, and diabatic motion, *Phys. Rev. Research* **2**, 033100 (2020), arXiv:1911.05667 [cond-mat.mes-hall].
- [31] See Supplementary Information, where the derivation of the Hall conductivity is documented and general gauge invariance is discussed.
- [32] D. Kaplan, T. Holder, and B. Yan, Unifying semiclassics and quantum perturbation theory at nonlinear order, to be published (2022a).
- [33] Y. Zhang, T. Holder, H. Ishizuka, F. de Juan, N. Nagaosa, C. Felser, and B. Yan, Switchable magnetic bulk photovoltaic effect in the two-dimensional magnet CrI_3 , *Nat. Commun.* **10**, 3783 (2019), arXiv:1903.06264 [cond-mat.mes-hall].
- [34] Y. Michishita and N. Nagaosa, Dissipation and geometry in nonlinear quantum transports of multiband electronic systems (2022).
- [35] D. Kaplan, T. Holder, and B. Yan, Twisted photovoltaics at terahertz frequencies from momentum shift current, *Phys. Rev. Research* **4**, 013209 (2022b), arXiv:2101.07539 [cond-mat.mes-hall].
- [36] T. Morimoto and N. Nagaosa, Topological nature of nonlinear optical effects in solids, *Sci. Adv.* **2**, e1501524 (2016), arXiv:1510.08112 [cond-mat.mes-hall].
- [37] J. E. Sipe and J. Zak, Geometric phase for electric polarization along 'rational' directions in crystals, *Phys. Lett. A* **258**, 406 (1999).
- [38] S. M. Young and A. M. Rappe, First Principles Calculation of the Shift Current Photovoltaic Effect in Ferroelectrics, *Phys. Rev. Lett.* **109**, 116601 (2012), arXiv:1202.3168 [cond-mat.mtrl-sci].
- [39] L. Z. Tan, F. Zheng, S. M. Young, F. Wang, S. Liu, and A. M. Rappe, Shift current bulk photovoltaic effect in polar materials—hybrid and oxide perovskites and beyond, *npj Comput. Mater.* **2**, 16026 (2016).
- [40] T. Holder, D. Kaplan, R. Ilan, and B. Yan, Mixed axial-gravitational anomaly from emergent curved spacetime in nonlinear charge transport (2021).
- [41] M. Tinkham, *Group Theory and Quantum Mechanics* (Dover Publications, 2003).
- [42] R. Bistritzer and A. H. MacDonald, Moiré bands in twisted double-layer graphene, *PNAS* **108**, 12233 (2011), arXiv:1009.4203 [cond-mat.mes-hall].
- [43] J. M. B. L. Santos, N. M. R. Peres, and A. H. Castro Neto, Continuum model of the twisted graphene bilayer, *Phys. Rev. B* **86**, 155449 (2012), arXiv:1202.1088 [cond-mat.mtrl-sci].
- [44] S. Carr, D. Massatt, S. B. Torrisi, P. Cazeaux, M. Luskin, and E. Kaxiras, Relaxation and domain formation in incommensurate two-dimensional heterostructures, *Phys. Rev. B* **98**, 224102 (2018), arXiv:1805.06972 [cond-mat.mes-hall].
- [45] W.-Y. He, D. Goldhaber-Gordon, and K. T. Law, Giant orbital magnetoelectric effect and current-induced magnetization switching in twisted bilayer graphene, *Nat. Commun.* **11**, 1650 (2020).
- [46] A. L. Sharpe, E. J. Fox, A. W. Barnard, J. Finney, K. Watanabe, T. Taniguchi, M. A. Kastner, and D. Goldhaber-Gordon, Emergent ferromagnetism near three-quarters filling in twisted bilayer graphene, *Science* **365**, 605 (2019), arXiv:1901.03520 [cond-mat.mes-hall].
- [47] U. Zondiner, A. Rozen, D. Rodan-Legrain, Y. Cao, R. Queiroz, T. Taniguchi, K. Watanabe, Y. Oreg, F. von Oppen, A. Stern, E. Berg, P. Jarillo-Herrero, and S. Ilani, Cascade of phase transitions and Dirac revivals in magic-angle graphene, *Nature* **582**, 203 (2020), arXiv:1912.06150

- [cond-mat.mes-hall].
- [48] J. Liu and X. Dai, Theories for the correlated insulating states and quantum anomalous hall effect phenomena in twisted bilayer graphene, *Physical Review B* **103**, 10.1103/physrevb.103.035427 (2021), arXiv:1911.03760 [cond-mat.str-el].
- [49] M. Lee, J. R. Wallbank, P. Gallagher, K. Watanabe, T. Taniguchi, V. I. Fal'ko, and D. Goldhaber-Gordon, Ballistic miniband conduction in a graphene superlattice, *Science* **353**, 1526 (2016), arXiv:1603.01260 [cond-mat.mes-hall].
- [50] H. Kim, N. Leconte, B. L. Chittari, K. Watanabe, T. Taniguchi, A. H. MacDonald, J. Jung, and S. Jung, Accurate Gap Determination in Monolayer and Bilayer Graphene/h-BN Moiré Superlattices, *Nano Letters* **18**, 7732 (2018), arXiv:1808.06633 [cond-mat.mes-hall].
- [51] A. Kerelsky, L. J. McGilly, D. M. Kennes, L. Xian, M. Yankowitz, S. Chen, K. Watanabe, T. Taniguchi, J. Hone, C. Dean, A. Rubio, and A. N. Pasupathy, Maximized electron interactions at the magic angle in twisted bilayer graphene, *Nature* **572**, 95 (2019).
- [52] J. Shi, G. Vignale, D. Xiao, and Q. Niu, Quantum Theory of Orbital Magnetization and Its Generalization to Interacting Systems, *Phys. Rev. Lett.* **99**, 197202 (2007), arXiv:0704.3824 [cond-mat.mes-hall].
- [53] The two-band part of this formula trivially vanishes, because neither v^x nor v^y have any diagonal terms in the incompressible phase.
- [54] A. I. Berdyugin, N. Xin, H. Gao, S. Slizovskiy, Z. Dong, S. Bhattacharjee, P. Kumaravadivel, S. Xu, L. A. Ponomarenko, M. Holwill, D. A. Bandurin, M. Kim, Y. Cao, M. T. Greenaway, K. S. Novoselov, I. V. Grigorieva, K. Watanabe, T. Taniguchi, V. I. Fal'ko, L. S. Levitov, R. K. Kumar, and A. K. Geim, Out-of-equilibrium criticalities in graphene superlattices, *Science* **375**, 430 (2022), arXiv:2106.12609 [cond-mat.other].
- [55] Y. Okazaki, T. Oe, M. Kawamura, R. Yoshimi, S. Nakamura, S. Takada, M. Mogi, K. S. Takahashi, A. Tsukazaki, M. Kawasaki, Y. Tokura, and N.-H. Kaneko, Quantum anomalous Hall effect with a permanent magnet defines a quantum resistance standard, *Nature Physics* **18**, 25 (2022).
- [56] Y. Gao, S. A. Yang, and Q. Niu, Field Induced Positional Shift of Bloch Electrons and Its Dynamical Implications, *Phys. Rev. Lett.* **112**, 166601 (2014), arXiv:1402.2538 [cond-mat.mes-hall].
- [57] S. S. Tsirkin and I. Souza, On the separation of Hall and Ohmic nonlinear responses, *SciPost Phys. Core* **5**, 39 (2022).
- [58] S. Lahiri, K. Das, D. Culcer, and A. Agarwal, Intrinsic nonlinear conductivity induced by the quantum metric dipole, , arXiv:2207.02178 (2022), arXiv:2207.02178 [cond-mat.mes-hall].
- [59] G. B. Ventura, D. J. Passos, J. M. B. Lopes dos Santos, J. M. Viana Parente Lopes, and N. M. R. Peres, Gauge covariances and nonlinear optical responses, *Phys. Rev. B* **96**, 035431 (2017), arXiv:1703.07796 [cond-mat.other].
- [60] D. J. Passos, G. B. Ventura, J. M. V. P. Lopes, J. M. B. L. d. Santos, and N. M. R. Peres, Nonlinear optical responses of crystalline systems: Results from a velocity gauge analysis, *Phys. Rev. B* **97**, 235446 (2018), arXiv:1712.04924 [cond-mat.other].
- [61] S. M. João and J. M. Viana Parente Lopes, Basis-independent spectral methods for non-linear optical response in arbitrary tight-binding models, *Journal of Physics Condensed Matter* **32**, 125901 (2020), arXiv:1810.03732 [cond-mat.other].
- [62] H. Rostami, M. I. Katsnelson, G. Vignale, and M. Polini, Gauge invariance and Ward identities in nonlinear response theory, *Annals of Physics* **431**, 168523 (2021), arXiv:2102.04425 [cond-mat.mes-hall].
- [63] B. A. Bernevig and T. L. Hughes, *Topological Insulators and Topological Superconductors* (Princeton University Press, 2013).
- [64] C. Aversa and J. E. Sipe, Nonlinear optical susceptibilities of semiconductors: Results with a length-gauge analysis, *Phys. Rev. B* **52**, 14636 (1995).

Supplementary information

REDUCTION OF THE KUBO FORMULA

In this section we give the derivation of the electric-field induced nonlinear correction via a Kubo formula. The details of the diagrammatic approach are listed in Refs. [30]. We specifically the insertion of finite lifetimes according to the prescription of Ref. [32], and employ the notation therein. We expand to order τ^0 , which represents the dissipation-less correction to the linear conductivity. In the diagrammatic picture, 4 diagrams contribute (may be insert these later). For simplicity, we consider here the case of $\sigma^{xx;y}$. An analogous expression can be derived for $\sigma^{yy;x}$. For compactness, we omit the Fermi occupation factor throughout. The total conductivity $\sigma^{xx;y}$ at order τ^0 reads,

$$\sigma^{xx;y} = \mathcal{W}^{xx;y} + \mathcal{V}^{xx;y}. \quad (S1)$$

$\mathcal{W}^{xx;y}$ contains contributions from two-photon vertices, while $\mathcal{V}^{xx;y}$ are three-legged diagrams. Parsing $\mathcal{W}^{xx;y}$,

$$\mathcal{W}_{\tau^0}^{xx;y} = -2 [\varepsilon^{-3} w^{xx}, v_y] - [\varepsilon^{-3} v^x, w^{xy}] = -2 [\varepsilon^{-3} v_y, w^{xx}] - [\varepsilon^{-3} v^x, w^{xy}]. \quad (S2)$$

Recall that $w^{xx} = 2i\Delta^x \mathcal{A}^x - [\varepsilon \mathcal{A}^x, \mathcal{A}^x] + i\varepsilon S^{xx}$. Furthermore, $w^{xy} = i\Delta^x \mathcal{A}^y + i\Delta^y \mathcal{A}^x - \frac{1}{2} [\varepsilon \mathcal{A}^x, \mathcal{A}^y] - \frac{1}{2} [\varepsilon \mathcal{A}^y, \mathcal{A}^x] + i\varepsilon S^{xy}$. $v^{x,y} = i\varepsilon \mathcal{A}^{x,y}$ (since only off-diagonal components are involved).

$$\begin{aligned} \mathcal{W}_{\tau^0}^{xx;y} = & -2i [\varepsilon^{-2} \mathcal{A}^y, 2i\Delta^x \mathcal{A}^x - [\varepsilon \mathcal{A}^x, \mathcal{A}^x] + i\varepsilon S^{xx}] - \\ & i [\varepsilon^{-2} \mathcal{A}^x, i\Delta^x \mathcal{A}^y + i\Delta^y \mathcal{A}^x - (1/2)[\varepsilon \mathcal{A}^x, \mathcal{A}^y] - (1/2)[\varepsilon \mathcal{A}^y, \mathcal{A}^x] + i\varepsilon S^{xy}]. \end{aligned} \quad (S3)$$

Terms may now be rearranged given the transposition properties of objects inside the commutator. For example, $[\varepsilon^{-2} \mathcal{A}^x, \Delta^x \mathcal{A}^y] = [\varepsilon^{-2} \mathcal{A}^y, \Delta^x \mathcal{A}^x]$. This stems from the fact that $\varepsilon_{nm}^2 = \varepsilon_{mn}^2$, but $\Delta_{nm}^x = -\Delta_{mn}^x$. Thus,

$$\begin{aligned} \mathcal{W}_{\tau^0}^{xx;y} = & 5 [\varepsilon^{-2} \mathcal{A}^y, \Delta^x \mathcal{A}^x] + [\varepsilon^{-2} \mathcal{A}^x, \Delta^y \mathcal{A}^x] + 2i [\varepsilon^{-2} \mathcal{A}^y, [\varepsilon \mathcal{A}^x, \mathcal{A}^x]] - 2 [\varepsilon^{-1} \mathcal{A}^y, S^{xx}] + \\ & \frac{i}{2} [\varepsilon^{-2} \mathcal{A}^x, [\varepsilon \mathcal{A}^x, \mathcal{A}^y] + [\varepsilon \mathcal{A}^y, \mathcal{A}^x]] - [\varepsilon^{-1} \mathcal{A}^x, S^{xy}]. \end{aligned} \quad (S4)$$

Next we turn our to $\mathcal{V}^{xx;y}$. As the expressions contain denominators ε_{nl} which depend on an intermediate index, we first isolate two cases of interest: $l = n, l = m$. The remainder are pieces for which $l \neq n, m$ and therefore are amenable to being written as proper commutators, as noted in the introduction. Since this section will involve explicit diagonal parts of the velocity operators $v_{nn}^{x,y}$ we restore the Fermi occupation factors. Firstly,

$$\mathcal{V}_{l=n,\tau^0}^{xx;y} = \frac{f_{nm}}{2\varepsilon_{nm}^4} v_{nm}^x v_{mn}^x v_{nn}^y + \frac{f_{nm}}{2\varepsilon_{nm}^4} v_{nn}^y v_{mn}^x v_{nm}^x \quad (S5)$$

Interchanging the summation on the second term ($n \leftrightarrow m$), gives,

$$\frac{f_{nm}}{2\varepsilon_{nm}^4} (v_{nm}^x v_{mn}^x (v_{nn}^y - v_{mm}^y)) = \frac{1}{2} \left[\frac{v^x}{\varepsilon^4} \Delta^y, v^x \right] = \frac{1}{2} \left[\frac{\mathcal{A}^x}{\varepsilon^2} \Delta^y, \mathcal{A}^x \right]. \quad (S6)$$

Next is the case of $l = m$,

$$\mathcal{V}_{l=m,\tau^0}^{xx;y} = -7 \frac{f_{nm}}{\varepsilon_{nm}^4} v_{nm}^x v_{mm}^x v_{mn}^y - 7 \frac{f_{nm}}{\varepsilon_{nm}^4} v_{nm}^y v_{mm}^x v_{mn}^x = 7 [\varepsilon^{-4} v^y \Delta^x, v^x] = 7 [\varepsilon^{-2} \mathcal{A}^y \Delta^x, \mathcal{A}^x] = -7 [\varepsilon^{-2} \mathcal{A}^y, \Delta^x \mathcal{A}^x]. \quad (S7)$$

The remaining terms, such that $l \neq n, m$ are,

$$\mathcal{V}_{l \neq n,m,\tau^0}^{xx;y,(1)} = -4 \frac{f_{nm}}{\varepsilon_{nm} \varepsilon_{nl}^3} v_{nm}^x v_{ml}^x v_{ln}^y - 2 \frac{f_{nm}}{\varepsilon_{nm}^2 \varepsilon_{nl}^2} v_{nm}^x v_{ml}^x v_{ln}^y - \frac{f_{nm}}{\varepsilon_{nm}^3 \varepsilon_{nl}} v_{nm}^x v_{ml}^x v_{ln}^y, \quad (S8)$$

while $\mathcal{V}_{l \neq n,m}^{xx;y,(2)}$ is the complex conjugate of $\mathcal{V}_{l \neq n,m}^{xx;y,(1)}$. Let us treat each term separately. After substituting $v^{x,y}$, and adding the complex conjugate the first term yields $-4 \frac{f_{nm}}{\varepsilon_{nm} \varepsilon_{nl}} v_{nm}^x v_{ml}^x v_{ln}^y = -4i [\mathcal{A}^x, [\varepsilon \mathcal{A}^x, \varepsilon^{-2} \mathcal{A}^y]]$. We break this term up into two pieces of equal prefactor, 2, and the first piece is replaced using a Jacobi identity. That is, $-2i [\mathcal{A}^x, [\varepsilon \mathcal{A}^x, \varepsilon^{-2} \mathcal{A}^y]] = 2i [\varepsilon^{-2} \mathcal{A}^y, [\mathcal{A}^x, \varepsilon \mathcal{A}^x]] + 2i [\varepsilon \mathcal{A}^x, [\varepsilon^{-2} \mathcal{A}^y, \mathcal{A}^x]]$. The other piece is written down differently.

Using the fact that $\varepsilon_{ml} = \varepsilon_{mn} + \varepsilon_{nl}$, $-2i [\mathcal{A}^x, [\varepsilon \mathcal{A}^x, \varepsilon^{-2} \mathcal{A}^y]] = -2i [\mathcal{A}^x, \varepsilon [\mathcal{A}^x, \varepsilon^{-2} \mathcal{A}^y]] + 2i [\mathcal{A}^x, [\mathcal{A}^x, \varepsilon^{-1} \mathcal{A}^y]]$. Adding this up once more gives,

$$-4i [\mathcal{A}^x, [\varepsilon \mathcal{A}^x, \varepsilon^{-2} \mathcal{A}^y]] = 2i [\varepsilon^{-2} \mathcal{A}^y, [\mathcal{A}^x, \varepsilon \mathcal{A}^x]] + 2i [\mathcal{A}^x, [\mathcal{A}^x, \varepsilon^{-1} \mathcal{A}^y]]. \quad (\text{S9})$$

The next term in Eq. (S8) is decomposed analogously.

$$-2 \frac{f_{nm}}{\varepsilon_{nm}^2 \varepsilon_{ln}^2} v_{nm}^x v_{ml}^x v_{ln}^y = 2i \left[\frac{\mathcal{A}^x}{\varepsilon}, [\varepsilon \mathcal{A}^x, \varepsilon^{-1} \mathcal{A}^y] \right] = -2i [\mathcal{A}^x, [\mathcal{A}^x, \varepsilon^{-1} \mathcal{A}^y]] - 2i [\varepsilon^{-1} \mathcal{A}^x, [\mathcal{A}^x, \mathcal{A}^y]] \quad (\text{S10})$$

The last term in Eq. (S8) is given by,

$$-\frac{f_{nm}}{\varepsilon_{nm}^3 \varepsilon_{nl}} v_{nm}^x v_{ml}^x v_{ln}^y = -i [\varepsilon^{-2} \mathcal{A}^x, [\varepsilon \mathcal{A}^x, \mathcal{A}^y]]. \quad (\text{S11})$$

We are now ready to assemble all the pieces we have. We combine,

$$\begin{aligned} & \mathcal{V}^{xx;y} + \mathcal{W}^{xx;y} = \\ & 5 [\varepsilon^{-2} \mathcal{A}^y, \Delta^x \mathcal{A}^x] + [\varepsilon^{-2} \mathcal{A}^x, \Delta^y \mathcal{A}^x] + 2i [\varepsilon^{-2} \mathcal{A}^y, [\varepsilon \mathcal{A}^x, \mathcal{A}^x]] - 2 [\varepsilon^{-1} \mathcal{A}^y, S^{xx}] + \\ & \frac{i}{2} [\varepsilon^{-2} \mathcal{A}^x, [\varepsilon \mathcal{A}^x, \mathcal{A}^y] + [\varepsilon \mathcal{A}^y, \mathcal{A}^x]] - [\varepsilon^{-1} \mathcal{A}^x, S^{xy}] + \frac{1}{2} \left[\frac{\mathcal{A}^x}{\varepsilon^2} \Delta^y, \mathcal{A}^x \right] - 7 [\varepsilon^{-2} \mathcal{A}^y, \Delta^x \mathcal{A}^x] + 2i [\varepsilon^{-2} \mathcal{A}^y, [\mathcal{A}^x, \varepsilon \mathcal{A}^x]] \\ & + 2i [\mathcal{A}^x, [\mathcal{A}^x, \varepsilon^{-1} \mathcal{A}^y]] - 2i [\mathcal{A}^x, [\mathcal{A}^x, \varepsilon^{-1} \mathcal{A}^y]] - 2i [\varepsilon^{-1} \mathcal{A}^x, [\mathcal{A}^x, \mathcal{A}^y]] - i [\varepsilon^{-2} \mathcal{A}^x, [\varepsilon \mathcal{A}^x, \mathcal{A}^y]]. \end{aligned} \quad (\text{S12})$$

We obtain,

$$\begin{aligned} & \mathcal{V}^{xx;y} + \mathcal{W}^{xx;y} = \\ & -2 [\varepsilon^{-2} \mathcal{A}^y, \Delta^x \mathcal{A}^x] + \frac{1}{2} [\varepsilon^{-2} \mathcal{A}^x, \Delta^y \mathcal{A}^x] - 2 [\varepsilon^{-1} \mathcal{A}^y, S^{xx}] + \frac{i}{2} [\varepsilon^{-2} \mathcal{A}^x, -[\varepsilon \mathcal{A}^x, \mathcal{A}^y] + [\varepsilon \mathcal{A}^y, \mathcal{A}^x]] + \\ & - [\varepsilon^{-1} \mathcal{A}^x, S^{xy}] - 2i [\varepsilon^{-1} \mathcal{A}^x, [\mathcal{A}^x, \mathcal{A}^y]]. \end{aligned} \quad (\text{S13})$$

This term contains several total derivatives, which are Fermi surface terms, and give rise to the recently proposed gravitational anomaly and intrinsic non-dissipative Hall effects [40, 56]. We remove them by observing that,

$$\partial_y [\varepsilon^{-1} \mathcal{A}^x, \mathcal{A}^x] = 2 [\varepsilon^{-1} \mathcal{A}^x, S^{xy}] + [\varepsilon^{-2} \mathcal{A}^x, \Delta^y \mathcal{A}^x] + [\varepsilon^{-1} \mathcal{A}^x, i[\mathcal{A}^y, \mathcal{A}^x]] \quad (\text{S14})$$

$$\partial_x [\varepsilon^{-1} \mathcal{A}^y, \mathcal{A}^x] = [\varepsilon^{-1} \mathcal{A}^x, S^{xy}] + [\varepsilon^{-1} \mathcal{A}^y, S^{xx}] - [\varepsilon^{-2} \mathcal{A}^y \Delta^x, \mathcal{A}^x] + [\varepsilon^{-1} \mathcal{A}^x, (i/2)[\mathcal{A}^x, \mathcal{A}^y]]. \quad (\text{S15})$$

By combining these identities with the symmetrization condition one finds,

$$\begin{aligned} & \sigma^{xx;y} = 2\partial_y [\varepsilon^{-1} \mathcal{A}^x, \mathcal{A}^x] - \partial_x [\varepsilon^{-1} \mathcal{A}^y, \mathcal{A}^x] + \\ & \frac{1}{2} [\varepsilon^{-2} \mathcal{A}^y, \Delta^x \mathcal{A}^x] - \frac{1}{2} [\varepsilon^{-2} \mathcal{A}^x, \Delta^y \mathcal{A}^x] + [\varepsilon^{-1} \mathcal{A}^x, S^{xy}] - [\varepsilon^{-1} \mathcal{A}^y, S^{xx}] + [\varepsilon^{-1} \mathcal{A}^x, (i/2)[\mathcal{A}^x, \mathcal{A}^y]]. \end{aligned} \quad (\text{S16})$$

In the above, we employed the identity that $\tilde{\Omega}^{xy,1} - \tilde{\Omega}^{yx,1} = \varepsilon \Omega^{ab}$, otherwise proven here [32]. We note that this form is fully compatible with the consistent separation of nonlinear response conductivity into Hall components carried out in Ref. [57]. We also note that the positional shift S^{xy} described here is related (while more general) to the quantum metric dipole, also recently shown to present an in-gap Hall conductivity [58].

GAUGE INVARIANCE OF THE DERIVED CORRECTION

The introduction of derivatives of the wavefunction in the expressions for $I_1 - I_3$ Eqs. (4)-(6) requires delicate handling of gauge transformations. The Bloch manifold of cell-periodic states is characterized by an invariance to the $U(1)^N$ transformation,

$$|n\mathbf{k}\rangle \rightarrow e^{-i\theta_n(k)} |n\mathbf{k}\rangle. \quad (\text{S17})$$

For notational ease, we suppress below the label \mathbf{k} , and refer to $|n\rangle$, as $|n\rangle = |n\mathbf{k}\rangle$. The Bloch periodic part of the Hamiltonian commutes with this gauge transformation since $[H(\mathbf{k}), f(k)] = 0$. The observables of optical response

are modified due to the gauge covariance of the states. The velocity operator $v^\alpha \rightarrow Uv^\alpha$, where $U_{nm} = e^{i\theta_{nm}}$, $\theta_{nm} = \theta_n - \theta_m$. Clearly, only diagonal components, such as those comprising $\Delta_{nm}^\alpha = v_{nn}^\alpha - v_{mm}^\alpha$, are automatically gauge invariant. Products such as $(v^\alpha)^\dagger v^\beta \rightarrow v^\alpha U^\dagger U v^\beta = v^\alpha v^\beta$ are gauge invariant. In this respect, the equations of optical response in the velocity gauge are manifestly gauge invariant, as they combine products of gauge covariant operators derived from the Hamiltonian. The issue of local $U(1)$ gauge invariance in the context of electromagnetism and optical response has recently been addressed, with gauge invariance formally proven [59–62]. Our primary focus, therefore, is to show that Eqs. (4)-(6) which involve *derivatives* of the Bloch periodic part of the electronic wavefunctions are also gauge invariant. The principle derivatives defining 2nd order optical response are [32]:

$$\mathcal{A}_{nm}^\alpha = \langle n | i\partial_\alpha | m \rangle \rightarrow \partial_\alpha \theta_n \delta_{nm} + e^{i\theta_{nm}} \langle n | i\partial_\alpha | m \rangle = e^{i\theta_{nm}} \mathcal{A}_{nm}^\alpha + \partial_\alpha \theta_n \delta_{nm} \quad (\text{S18})$$

$$\lambda_{nm}^{\alpha\beta} = \frac{1}{2} \langle n | i\partial_\alpha \partial_\beta | m \rangle + (\text{c.c.}, n \leftrightarrow m) \rightarrow e^{i\theta_{nm}} \lambda_{nm}^{\alpha\beta} + \frac{ie^{i\theta_{nm}}}{2} (\mathcal{A}_{nm}^\alpha \partial_\beta \theta_{nm} + \mathcal{A}_{nm}^\beta \partial_\alpha \theta_{nm}), \quad n \neq m. \quad (\text{S19})$$

We define objects which are gauge *covariant* as those which transform as $A_{nm} \rightarrow A_{nm} e^{i\theta_{nm}}$. Consequently, combinations of the form $A_{nm} A_{mn}$ are manifestly gauge *invariant* since they transform like the velocity operator, as shown above, or $e^{i\theta_{nm}} A_{nm} e^{i\theta_{mn}} A_{mn} = A_{nm} A_{mn}$. Generally, for *any* two covariant objects A, B , the commutator of the two satisfies,

$$[A, B]_{nm} \rightarrow e^{i\theta_{nm}} [A, B]_{nm}, \quad (\text{S20})$$

rendering its diagonal part gauge invariant. This follows from the definition introduced in the main text, $[A, B]_{nm} = \sum_{l \neq n, m} A_{nl} B_{lm} - (A \leftrightarrow B)$. We now prove that the quantity $S_{nm}^{\alpha\beta}$, $n \neq m$ is gauge covariant, which appears in I_2 , of Eq. (5). We note that $S^{\alpha\beta}$ consists of two portions: $\lambda_{nm}^{\alpha\beta}$ and the Hadamard product, $\frac{i}{2} \mathcal{A}_{nm}^\alpha \delta_{nm}^\beta + (\alpha \leftrightarrow \beta)$. Tackling the latter first,

$$\frac{i}{2} \mathcal{A}_{nm}^\alpha \delta_{nm}^\beta \rightarrow \frac{i}{2} e^{i\theta_{nm}} \mathcal{A}_{nm}^\alpha \partial_\beta \theta_{nm}. \quad (\text{S21})$$

To uncover the transformation properties of $\lambda_{nm}^{\alpha\beta}$ for $n \neq m$, we first observe that under $|m\rangle \rightarrow e^{i\theta_m} |m\rangle$, $\partial_\alpha \partial_\beta |m\rangle \rightarrow e^{i\theta_m} (i\partial_\alpha \theta_m |\partial_\beta m\rangle + i\partial_\beta \theta_m |\partial_\alpha m\rangle + |\partial_\alpha \partial_\beta m\rangle)$. We explicitly remove the term $e^{i\theta_m} \partial_\alpha \partial_\beta \theta_m |m\rangle$ since we assume that $n \neq m$ and this contribution must vanish when projected back onto the Bloch states. Multiplying on the left with $i \langle n |$, we find that,

$$\lambda_{nm}^{\alpha\beta} \rightarrow \frac{e^{i\theta_{nm}}}{2} \lambda_{nm}^{\alpha\beta} + \frac{i}{2} e^{i\theta_{nm}} \mathcal{A}^\alpha \partial_\beta \theta_{mn} + (\alpha \leftrightarrow \beta). \quad (\text{S22})$$

It follows that the sum of the objects,

$$\frac{1}{2} \lambda_{nm}^{\alpha\beta} + \frac{i}{2} \mathcal{A}_{nm}^\alpha \delta_{nm}^\beta + (a \leftrightarrow b) \rightarrow e^{i\theta_{nm}} \left(\frac{1}{2} \lambda_{nm}^{\alpha\beta} + \frac{i}{2} \mathcal{A}_{nm}^\alpha \delta_{nm}^\beta \right) + (a \leftrightarrow b), \quad (\text{S23})$$

With the θ dependent part explicitly cancelling as it appears with opposite indices θ_{nm} vs θ_{mn} . Lastly, the triple commutator introduced in Eq. (6) transforms using the rules outlined above for commutators. The product reads,

$$[\mathcal{A}^x, i[\mathcal{A}^x, \mathcal{A}^y]]_{nn} = i\mathcal{A}_{nm}^x [\mathcal{A}^x, \mathcal{A}^y]_{mn} - i[\mathcal{A}^x, \mathcal{A}^y]_{nm} \mathcal{A}_{mn}^x \rightarrow e^{i\theta_{nm}} \mathcal{A}_{nm}^x e^{i\theta_{mn}} [\mathcal{A}^x, \mathcal{A}^y]_{mn} - (\text{c.c.}) = [\mathcal{A}^x, i[\mathcal{A}^x, \mathcal{A}^y]]_{nn}. \quad (\text{S24})$$

Here, we used the fact that commutator as defined does not sum over any diagonal contributions and off-diagonal parts of the Berry connection transform according to Eq. (S18).

QUANTIZATION OF THE LINEAR KUBO FORMULA FOR THE IQHE

The linear response contribution at zero frequency reads [63],

$$\sigma^{xy} = \frac{ie^2}{L_x L_y \hbar} \sum_{n, m} f_{nm} \frac{v_{nm}^x v_{mn}^y}{\varepsilon_{nm}^2}. \quad (\text{S25})$$

Here the sum n, m runs over all bands (occupied and empty) including the degenerate manifold of each occupied Landau level. Based on the identities defined in the main text for the velocity matrix elements, we have,

$$v_{nm}^x v_{mn}^y = \frac{i\hbar\omega_c}{2M} (\sqrt{m+1}\delta_{n, m+1} - \sqrt{m}\delta_{n, m-1}) (\sqrt{m+1}\delta_{n, m+1} + \sqrt{m}\delta_{n, m-1}). \quad (\text{S26})$$

The energy difference (measured in frequency units) is $\varepsilon_{nm} = \omega_c(n - m)$. The only surviving terms above are products of equal delta functions. Thus,

$$\frac{v_{nm}^x v_{mn}^y}{\varepsilon_{nm}^2} = \frac{i\hbar\omega_c ((m+1)\delta_{n,m+1} - m\delta_{n,m-1})}{2M \omega_c^2 (n-m)^2}. \quad (\text{S27})$$

Assume now that there are ν occupied bands, which are each $N = \frac{eBL_x L_y}{h}$ -fold degenerate. The linear conductivity Eq. (S25) has a global Fermi occupation factor difference $f_{nm} = f_n - f_m$. In the bulk of the quantum Hall fluid, a fully flat Landau band is either completely occupied or completely empty. Therefore, f_{nm} is non-zero only in the cases $n = \nu, m = \nu + 1, f_{nm} = 1$, and $n = \nu + 1, m = \nu, f_{nm} = -1$. By further accounting for the degeneracy, we have,

$$\begin{aligned} \sigma^{xy} &= \frac{ie^2}{L_x L_y \hbar} \sum_{n,m} f_{nm} \frac{v_{nm}^x v_{mn}^y}{\varepsilon_{nm}^2} = \\ &= \frac{eBL_x L_y}{h} \times \left[\frac{ie^2}{L_x L_y \hbar} \frac{i\hbar\omega_c}{2M} \left(\frac{-(\nu+1)}{\omega_c^2} - \frac{(\nu+1)}{\omega_c^2} \right) \right] = \frac{e^2}{h} (\nu + 1). \end{aligned} \quad (\text{S28})$$

σ^{xy} is therefore quantized by the number of filled Landau levels.

TWO BAND MODELS

The simplest approximation that can be made consists of a two band topological model with non-vanishing Berry curvature. We show here that a fundamental condition for the emergence of our derived correction is the presence of nonlinear terms. A minimal Hamiltonian for the which produces a non-zero correction reads,

$$H = (M + 2 - \cos(k_x) - \cos(k_y))\sigma_z + (\sin(k_x) + \alpha L_x) \sigma_x + (\sin(k_y) + \beta L_y) \sigma_y \quad (\text{S29})$$

$$L_x = \sin(k_x) \sin(k_y), \quad L_y = \sin(k_x) \cos(k_y), \quad (\text{S30})$$

which is a model for a single Dirac cone with nonlinear terms represented by L_x, L_y . Here, σ are Pauli matrices in an orbital basis. When $\alpha = \beta = 0$, the model retains inversion symmetry, which is defined by $P = \sigma_z(k \rightarrow -k)$. This remains true when $\alpha = 0$ alone, since L_y is odd under $(k \rightarrow -k)$. The model is topological for all $-2 < M < 0$ with Chern number $C_N = -1$, and is trivial otherwise. The nonlinearities L_x, L_y do not merely break inversion and mirror symmetries remaining mirror but add higher derivatives of the Hamiltonian, i.e., $w^{ab} = \partial_a \partial_b H_0$, and induce a correction to the current operator, according to Eq. (1). In the absence of non-linearities, sum rules [64], notably that the fact that $\partial_a v_{nm}^b = i[r^a, v^b]_{nm} + i v_{nm}^b \delta_{nm}^a + i r_{nm}^a \Delta_{nm}^b$ emerge, enforcing cancellations between terms and nulling the correction. In Fig. S1(b), we show the magnitude of the correction as a function of of the mass parameter M of the model. The response diverges as $M \rightarrow 0$ due to the presence of ε_{nm}^{-n} , $n > 1$ in all terms. Unlike the Berry curvature, the flux of this expression, i.e. the integral $\sim \int dk \varepsilon^{-n} k$ does not equal a constant but decays as k^{-3} in the leading order. This makes the correction fundamentally different from the Berry curvature, as it is highly singular in the limit $k \rightarrow 0$ for a vanishing mass. The corrections are sensitive to the topology of the system, as shown in Fig. S1(b). In the non-topological case ($M > 0$), with vanishing total Berry phase, the corrections decay roughly as $M^{-3/2}$ while for $M < 0$, the decrease is of the form M^{-1} , indicating a slower suppression. The momentum space distribution is also different for the two cases. In Figs. S1(c-d) we plot the momentum space density of the terms $I_1 - I_3$ (Eqs. (4)-(6)). In the trivial case ($M > 0$, Fig. S1(d)), the divergence around the Γ point of the model is clearly apparent, while when $M < 0$ the density is diffused across a broader region in momentum space, with the peak way from the Γ point. As stated above, in the 2-band limit, I_3 (Eq. (6)) cannot contribute, and the non-linearity is most significantly encountered for the velocity shift I_1 (Eq. (4)).

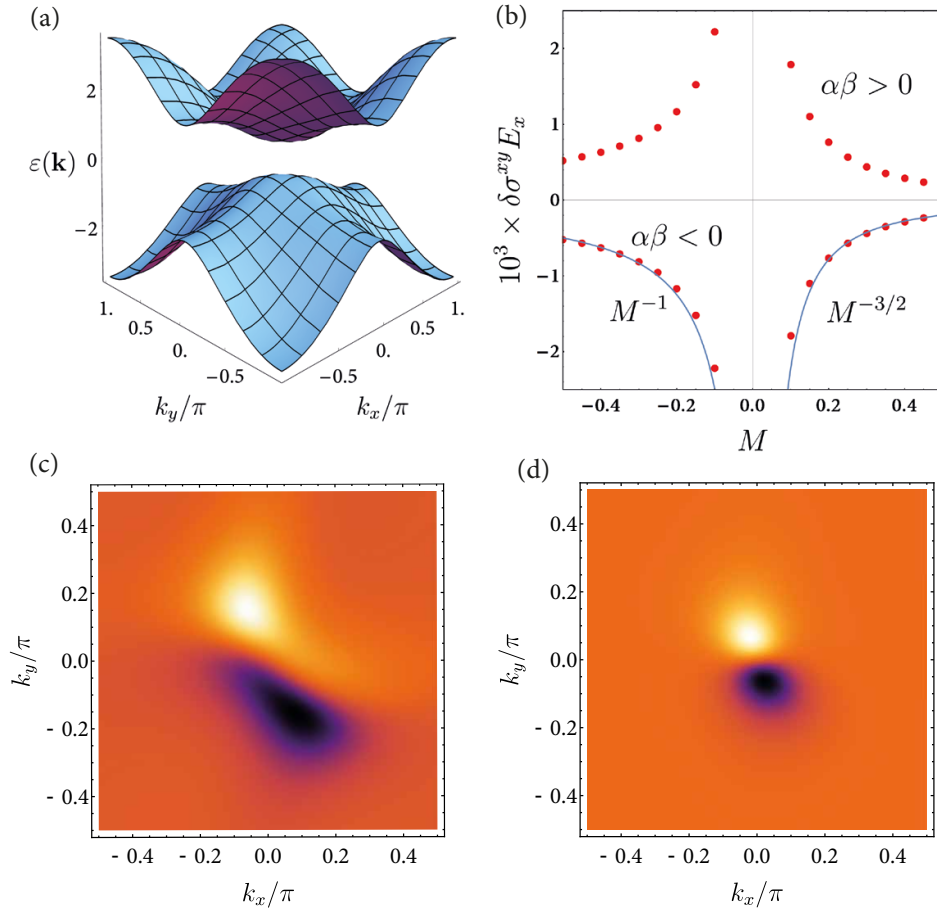


Figure S1. Nonlinear correction to the anomalous Hall conductivity of a gapped Dirac cone. (a) A two band model (Eq. (S30)) in the topological phase, when $M = -0.5$. (b) Magnitude of the correction $\delta\sigma^{xy}$ to the Hall conductivity, for $E_x = 1$. The sign of the correction depends on the sign of the product $\alpha\beta$. In the topological phase ($M < 0$), the correction decays like M^{-1} , while in the trivial phase ($M > 0$) it decreases with $M^{-3/2}$. (c-d) Momentum space distribution of $I_1 - I_3$ (Eqs. (4)-(6)) for the topological phase (c) and the trivial phase (d)